mathematics

Article

Developing a Spine Internal Rotation Angle Measurement System Based Machine Learning Using CT Reconstructed X-ray Anteroposterior Image

Tae-Seok Kang and Seung-Man Yu *

Department of Radiologic Science, College of Medical Sciences, Jeonju University, Jeonju 55069, Republic of Korea
* Correspondence: ysm9993@jj.ac.kr; Tel.: +82-63-220-2382

Abstract: The purpose of this study was to develop a predictive model for estimating the rotation angle of the vertebral body on X-ray anteroposterior projection (AP) image by applying machine learning. This study is intended to replace internal/external rotation of the thoracic spine (T-spine), which can only be observed through computed tomography (CT), with an X-ray AP image. 3-dimension (3D) T-spine CT images were used to acquired reference spine axial angle and various internal rotation T-spine reconstructed X-ray AP image. Distance from the pedicle to the outside of the spine and change in distance between the periphery of the pedicle according to the rotation of the spine were designated as main variables using reconstructed X-ray AP image. The number of measured spines was 453 and the number of variables for each spine was 13, creating a total of 5889 data. We applied a total of 24 regression machine learning methods using MATLAB software, performed learning with the acquired data, and finally, the Gaussian regression method showed the lowest RMSE value. X-rays obtained with the phantom of the human body tilted by 16 degrees showed results with reproducibility within the RMSE range.

Keywords: scoliosis; X-ray image; machine learning; computed tomography

MSC: 90-08

check for updates

Citation: Kang, T.-S.; Yu, S.-M. Developing a Spine Internal Rotation Angle Measurement System Based Machine Learning Using CT Reconstructed X-ray Anteroposterior Image. *Mathematics* **2022**, *10*, 4781. https://doi.org/10.3390/math10244781

Academic Editors: Xianye Ben, Peng Zhang, Tao Lei, Lei Chen and Junlin Hu

Received: 28 October 2022
Accepted: 13 December 2022
Published: 15 December 2022

1. Introduction

Adolescent idiopathic scoliosis (AIS) is a disease in which the spine twists and curves laterally with the column of the spine curved into a 'C-shape' or 'S- shape' [1,2]. Its occurrence is caused by several factors, such as genetics, structural elements of the spine, paravertebral musculature, metabolic & chemical factors, endocrine and central nervous system. However, studies on the effects of sedentary life, such as office workers and students living in a chair, are also being conducted [3,4]. In general, the diagnosis of scoliosis is made when the angle of the spine is evaluated to be more than 10° on the posterior-anterior radiograph related to the rotation of the spine [5,6]. Although scoliosis is known as a disease in which the column of the spine is bent outward on the coronal plane, in reality, when a three-dimensional spinal deformity occurs, the forehead, sagittal plane, and transverse plane are changed in spinal alignment [7].

To quantify the severity of AIS in scoliosis patients, the Cobb's angle is measured [8]. However, this method is limited in assessing sagittal and coronal spine curvature. For example, right scoliosis with respect to the coronal plane can cause a clockwise rotation of the vertebral body, whereas left scoliosis on the coronal plane causes a counterclockwise rotation [9]. Thus, recent studies have used various approaches to better understand AIS as a three-dimensional state [10–12]. An X-ray anteroposterior (AP) projection image is a two-dimension (2D) image viewed from the front. It is suitable for measuring the angle between the forehead and the sagittal plane of the spine. However, it cannot be used to accurately measure the rotation angle in the horizontal plane. Due to these limitations, studies conducted so far have mainly evaluated Cobb's Angle, the angle of inclination of the spine on the coronal plane, to determine a treatment effect [13–15]. When evaluating spinal rotation, the rotational deformation of the vertebral body in the plane due to scoliosis has a clinically significant meaning in an orthodontic procedure [16–18]. If internal spine rotation is not corrected, scoliosis recurrence occurs. Conversely, even a slight reduction in rotation can significantly improve scoliosis expressed in radiographs [19]. Therefore, measurement of internal rotation of the spine has an important meaning in the prognosis and treatment of scoliosis. For example, inaccurate evaluation of spine rotation during pedicle screw surgery can lead to misplacements that risk spinal cord injury. Recent studies have shown that the coupled relationship between rotation and lateral motion of the spine may provide insight into hallmarks of scoliosis [20,21]. The most accurate way to evaluate an internal rotation of the spine is to use computed tomography (CT) since CT can provide accurate phase information [22]. Attempts have been made to accurately measure the internal rotation of the spine using CT with various methods, such as the experiment of Stoke and Ho et al. [16,18]. Spinal rotation evaluation using CT has the advantage of evaluating the rotation of the spine accurately. However, most patients acquire the image while lying on a patient table during the CT image acquisition process. Since the patient's spine is not affected by gravity, information on spinal rotation that does not accurately reflect the patient's pathological environment due to muscle relaxation is provided [23]. In addition, CT images have limitations in that the burden of periodic examination of the spine before and after surgery is high due to its higher radiation dose than general X-rays. In addition, its examination cost is high [24]. Measuring the rotation angle of the vertebral body on an X-ray image has advantages. It can be examined more easily than a CT scan. It also reflects the degree of rotation of the spine under the influence of gravity. In addition, evaluating the rotation of the spine based on an X-ray image of the patient in a standing position is essential for accurate evaluation of the internal spine rotation of the patient.

On the other hand, CT images have the advantage of reformatting images identical to those of general X-rays by reconstructing the rotation angle of the spine in multiple directions based on previously acquired images using 3D medical software [25]. In other words, artificial spinal rotation can be performed with a CT image in 3D medical software and an X-ray image reflecting the internal rotation spine can be acquired. Therefore, the same image can be acquired without actually examining the X-ray AP image of the thoracic spine (T-Spine) that we want to know in this study, and a lot of data can be produced through this information. After reconstruction of image data obtained by rotating the vertebral body at various angles in 3D based on CT-imaged images into 2D X-ray simple images, the rotation angle of the spine could be predicted by machine learning. In addition, if various variables, such as the size of the spine and the lateral inclination angle of the spine, are applied by configuring the optimal parameters, it is possible to create a model that can predict the rotation angle of the vertebral body more accurately.

Therefore, the purpose of this study was to develop a spinal rotation angle measurement system using X-ray anteroposterior images. Variables to be used in the predictive model were extracted by measuring specific anatomical structures expressed in the spine as 2D X-ray images reconstructed from 3D CT spine images on a horizontal plane with left and right rotation angles of each vertebral body. In addition, we tried to develop a predictive model for estimating the rotation angle of the vertebral body on X-ray AP image by applying machine learning.

2. Materials and Methods

2.1. Experiment Subjects and 3D Computed Tomography Data Acquisition

CT 3D images obtained from 29 volunteers in their 20s were used as primary data in the experiment. Volunteers of this study were fully informed about this study. They provided informed consent to participate in the study. This study was approved by our Bioethics Committee (approval number: GU-2017-HRa-06-02).

3D CT images data of all volunteers of were acquired using a CT image device (Optima 660 General Electrics, New York City, State of New York, USA) from C-spine to L-spine. CT imaging scan parameters were set as follows: tube voltage, 120 kVp; tube current, 500 mA; pitch, 1.0; and reconstruction resolution, 512 × 512. 3D CT images were backed up as a Dicom file. The workflow from 3D CT data acquisition to the developed final prediction model in this study is presentative in Figure 1.

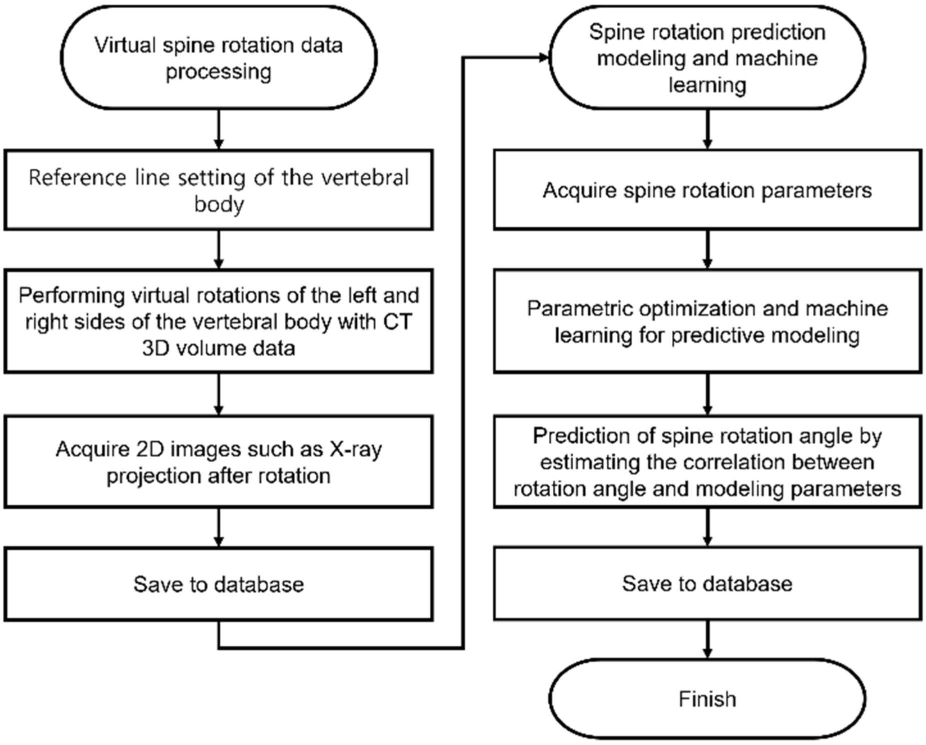

Figure 1. Machine Learning Workflow.

Spine 3D data were transmitted to a 3D medical image processing software (Infinity Korea, South Korea) to measure the internal rotation angle used for the machine running reference value. Afterward, the 3D spine was rotated at a certain angle in the direction of the long axis of the spine to induce artificial internal rotation of the spine and to reform the 2D X-ray AP projection image. We measured the length and angle of the reference anatomical structure we set using the obtained artificial inner rotation 2D X-ray AP projection image (Figure 2).

The artificial reconstructed 2D X-ray images' spine rotation angle, which was artificial internal rotation, was calculated by adding rotation angles in left and right directions from the reference angle measured with the CT axial image. A predictive model of spine rotation was developed using machine learning techniques with the obtained spine rotation angle and variables that we set.

2.2. Raw Data Acquisition and Measurement Variables of Spine Rotation Using 3D CT Data

In order to measure a measurement variable, the change in the projected 2D X-ray image structure according to the rotation of the spine, an accurate reference angle measurement must first be made from a transaxial image of the spine obtained by a CT image. The reference spine axis angle (RSAA) is the reference measured from T3 to T12 of 29 images of volunteers. Its measurement method is shown in Figure 2.

In this study, we measured RSAA by referring to Stokes' measurement method (Stokes et al., 1986). First, by setting center points of the pedicles on left and right sides of the spine, a line (a) connecting the pedicles on both sides was set. A vertical virtual line (b) was then set. The final RSAA was measured by measuring the angle formed with the line (c) that was perpendicular to the horizontal line of the image. The 2D X-ray AP projection image reflected RSAA as it was reconstructed. The distance between structures at the measurement reference line determined in Figure 2 was then measured (Figure 3).

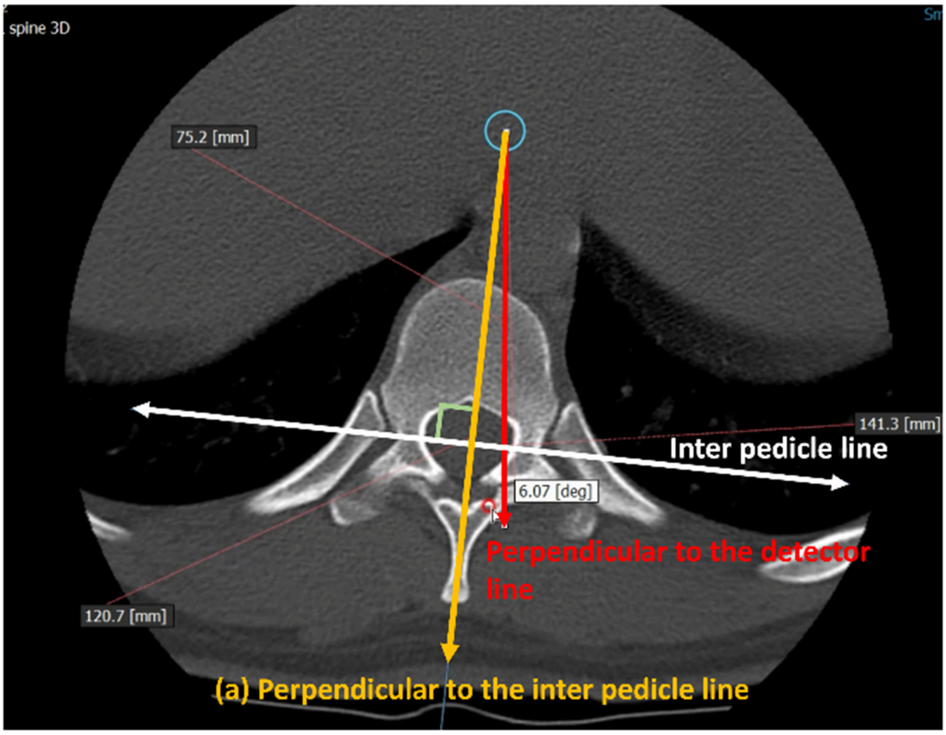

Figure 2. Measurements of reference spine axis angle (the basis for the spine) and spine variables. The most crucial line (a) is established by setting the center of the pedicle by checking the upper and lower tomography images of the spine trans-axial image and tracking it from the starting point of the pedicle. The image measures the degree of rotation of the spine concerning the pedicle on the horizontal plane of the CT. It shows a 6.07° clockwise rotation.

By applying the method of projecting CT scan data, a 3D image, onto one reference plane, it can be reconstructed into an image of a two-dimensional structure, such as an X-ray image. It is possible to measure or evaluate geometric structures. We obtained basic data extracted from the 2D image by setting lengths and angles F of A, B, C, and D as variable parameters for measuring the angle of rotation of the vertebral body. Their baseline measurements were performed as follows. First, the baseline on the transverse plane was set by setting the baseline parallel to the vertebral edge at the most convex center of the pedicle. Afterward, the distance (A) from the line connecting the outer upper and lower edges of the spine body to be measured to the external centerline of the pedicle was designated as the primary variable. In addition, the width distance (B) between pedicles was set as the distance from the outer margin of the pedicle on the baseline to the inner margin of the pedicle. The distance (C) between the lateral margin on the opposite side of the vertebrae from the endpoint of B was set. The longitudinal length (D) of the vertebral body is the length of the upper and lower margins of the spine. In addition, the angle (F) formed by the inclination of the spine and the baseline on the transverse plane was designated as a parameter for machine learning. Eight data per spine were acquired by artificially rotating each vertebra in the spine CT image data internally and externally five degrees using variables specified. Machine learning was performed to develop a predictive model by acquiring two-dimensional X-ray AP images for each rotation angle and using spine's prediction parameters and internal rotation as result values. To develop the predictive model, a machine learning toolbox of MATLAB (2020a, Mathworks, Natick, MA, state of Massachusetts, USA) was used. The performance of the final predictive model was evaluated with the Gaussian regression method.

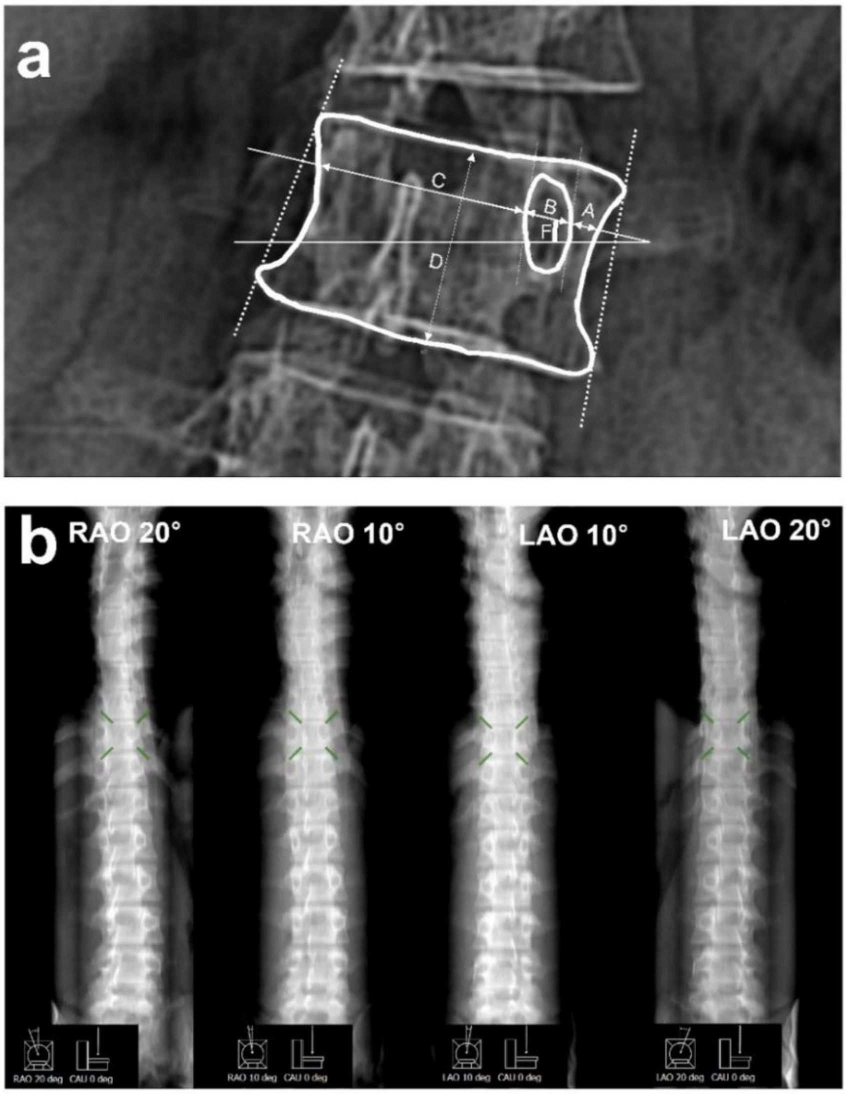

Figure 3. Measurements of reference spine axis angle (the basis of the spine) and spine variables. (**a**) is the measurement method of the spine variables by reconstructing a 2D X-ray projection image reflecting RSAA as it is, (**b**) The image is a 2D X-ray projection image projected by artificially rotating the 3D CT data. The RAO means right anterior oblique rotation view of the spine and LAO means left rotation.

2.3. Predictive Model Reproducibility Experiment

For the reproducibility experiment of the developed spine rotation prediction model, we artificially rotated a human phantom and compared the rotation angle of the spine with the value expressed by the prediction model. As shown in Figure 3, the human phantom with a shape similar to that of human vertebrae was taken in a left posterior oblique posture of 16 degrees. X-ray was then performed. The X-ray exposure field was set to include all T-spines of the phantom. The distance from the X-ray source to the image receptor was set to be 110 cm. Images were acquired with a digital radiography detector. Images obtained in this way were measured on the T-spine 7 by the same method as the values set as parameters of the prediction model and entered into the developed machine learning algorithm. The actual rotation angle and the predicted value were then compared (Figure 4).

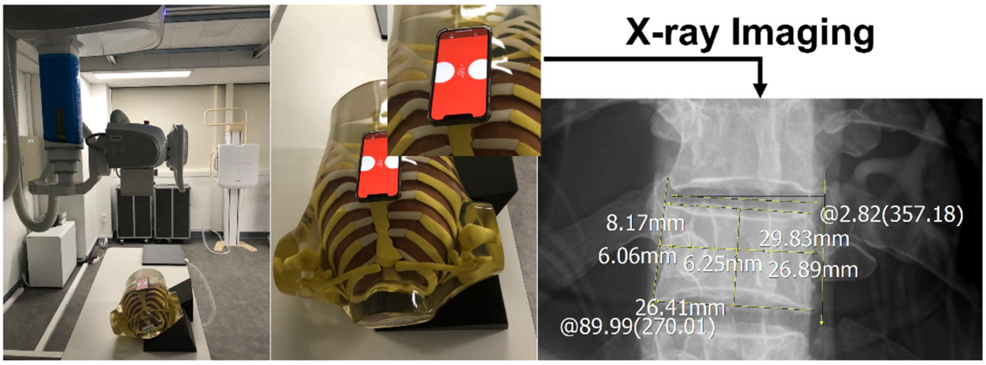

Figure 4. Predictive model reproducibility experiment. Experiment to acquire an X-ray image by rotating the phantom of the manikin by 16 degrees.

2.4. Gaussian Process Algorithm Showing Minimum RMSE Value

An appropriate inference process is required for the mean and covariance function $k(x,\ x')$. As in the formula below, use a hierarchical prior with mean and covariance functions parameterized by the hyperparameters of the Gaussian Process (GP).

$$f\ \sim GP(m,k) \tag{1}$$

$$m(x) = ax^2 + bx + c \tag{2}$$

$$k(x,\ x') = \sigma^2 \exp\left(-\frac{(x-x')^2}{2l^2}\right) + \sigma_n^2 \delta_{ii'} \tag{3}$$

At this time, set the hyperparameter set as $\theta = \left[a,\ b,\ c,\ \sigma_{y},\ \sigma_n,\ l\right]$. Given the measured data, a function f representing is learned. This function has a confidence interval or error bar as a probability model.

$$Data\ : D = [x,y] \tag{4}$$

The Gaussian Process distribution is organized by the mean function and the covariance function, and if the two spaces exactly match, it becomes an infinite dimensional quantity.

$$p(f) = f(x)\ \ \sim\ GP(m,k) \tag{5}$$

The above probability is subjected to Bayesian regression.

$$p(f|D) = \frac{p(f)p(D|f)}{p(D)} \tag{6}$$

The following formula is calculated for all existing data points to prepare for the Gaussian Process Regression.

$$K = \begin{pmatrix} K(x_{1,}x_1)\ K(x_1,x_2) & \cdots & K(x_{1,}x_n) \\ \vdots & \ddots & \vdots \\ K(x_{n,}x_1)\ K(x_n,x_2) & \cdots & K(x_{n,}x_n) \end{pmatrix}, \\ K_* = [K(x_*,x_1)\ K(x_*,x_2)\ldots\ (x_*,x_n)\ ] \quad K_{**} = K(x_*,x_*) \tag{7}$$

The diagonal element of K is $\sigma_f^2 + \sigma_n^2$, and the elements at the end of the off-diagonal elements have a value close to 0 as x spans a sufficiently large domain.

3. Results

To develop a predictive model for this experiment, T-spine was measured for spine data of 19 adults. The number of measured spines was 453 and the number of variables for each spine was 13, creating a total of 5889 data. The overall overview of the raw data used in machine learning is summarized in Table 1.

Table 1. Results of parameter setting/measurement method and data acquisition range.

Parameters	Measurement Methods	Data Acquisition Range
RSAA [1]	✓ angle (perpendicular to the inter pedicle line—perpendicular to the detector line) ✓ angle (perpendicular to the inter pedicle line—horizontal to the detector line)	−22.3–24.19°
A	✓ outer line of the center of the pedicle—line connecting the lateral upper and lower ends of the vertebral body	0.15–11.30 mm
B	✓ pedicle outer edge—pedicle inner edge	1.03–11.11 mm
C	✓ pedicle inner edge—line connecting the lateral upper and lower ends of the vertebral body	14.38–35.44 mm
D	✓ the midpoint of the upper spine line—center of the lower line of the spine	12.54–30.13 mm
F	✓ an imaginary line connecting A to C (the upper line of the vertebral body)—transverse plane	−7.44–4.9°

[1] reference spine axis angle.

For the data generated in this way, RSAA was set as the result value and the regression analysis prediction model method was performed using the machine learning method. Finally, Gaussian regression analysis was performed. The model that showed the lowest RMSE (root mean square error for validation) value was selected as the final prediction model.

For the development of the prediction model, the following steps were used. In step 1, spine number, A distance, B distance, C distance, and F angle were used as input to perform the step of processing data suitable for training the model. After that, data were processed in a form suitable for training the model and stored as predictors (measured values). The RSAA value, the measured rotation angle of each data, is stored as the response (actual value). Related coding is shown below:

```
inputTable = trainingData
predictorNames = 'spine number', 'A Distance', 'B Distance', 'C Distance', 'Pedicle line angle(F Angle)';
predictors = inputTable(:, predictorNames);
response = inputTable.Rotation_angle;
isCategoricalPredictor = [false, false, false, false, false];
```

In step 2, cross validation was performed for each data. For training the model, an object 'cvp' of cv partition that defines a non-stratified random partition was created to be used for 27-fold cross validation on the actual value of the response size and calculate the predicted value. Related coding is shown below:

```
KFolds = 27;
cvp = cvpartition(size(response, 1), 'KFold', KFolds);
validationPredictions = response;
```

After repeatedly performing cross-validation on 1 to 27 data, a multiple precedence algorithm was specified as an option and the model was trained. Related coding is as follows:

```
for fold = 1:KFolds
trainingPredictors = predictors(cvp.training(fold),:);
trainingResponse = response(cvp.training(fold),:);
foldIsCategoricalPredictor = isCategoricalPredictor;
```

The regression model was trained according to the multiple antecedent algorithm based on the training data including the spine-related input information as follows:

```
concatenatedPredictorsAndResponse = trainingPredictors;
concatenatedPredictorsAndResponse.Rotation_angle = trainingResponse;
linearModel = stepwiselm( ...
concatenatedPredictorsAndResponse, ...
'linear', ...
'Upper', 'interactions', ...
'NSteps', 1000, ...
'Verbose', 0);
```

After that, the resulting structure is generated using the prediction function as in the following coding.

```
linearModelPredictFcn = @(x) predict(linearModel, x);
validationPredictFcn = @(x) linearModelPredictFcn(x);
validationPredictors = predictors(cvp.test(fold),:);
foldPredictions = validationPredictFcn(validationPredictors);
validationPredictions(cvp.test(fold),:) = foldPredictions;
```

In step 3, TrainedModel (trained regression model) was returned. The validation predicted value of trainedModel (trained regression model) was also returned. After that, Validation RMSE was evaluated.

```
validationRMSE = sqrt(nansum((validationPredictions − response).^2)/ numel (response(isNotMissing)));
```

The value of RMSE was calculated with the following equation:

$$RMSE = \sqrt{\frac{1}{n}\sum_{i=1}^{n}(\text{Reference spine axis angle value} - \text{Expect spins axis angle value})^2} \quad (8)$$

4. Discussion

Scoliosis is a disease in which the vertebral column is deformed into an S shape. Still, the disease caused by the morphological deformity of the ribs as the spine is in the internal rotation is also considered clinically meaningful. Spinal rotation measurement provides critical information in determining a patient's surgery and performing pedicle screw operation [26]. In addition, since the degree of rotation of the spine acts as an essential index for diagnosing the treatment progress after surgery, the evaluation of rotation of the spine provides very informative clinical information [27,28]. The evaluation of spinal rotation through CT is the most accurate method among existing methods [29]. The CT image from which 3D volume data are acquired has the advantage of accurately measuring the angle and length of the spine in three reference planes: A coronal plane, a sagittal plane, and a transverse plane. However, CT increases the patient's radiation exposure. It also has a limitation in that the examination cost is more expensive than general X-ray. Therefore, we produced self-produced data using machine learning and developed a method to estimate and measure the spine's degree of left and right rotations using only X-ray images as CT information. As a result, it was possible to overcome limitations of CT examination with only X-ray images and measure left and right rotation angles. In other words, by using CT volume data to accurately measure the information on the rotation of the spine and by rotating the vertebral body cross-section image, self-produced data were produced as an X-ray image. We then obtained an algorithm optimized by machine learning using the generated data to predict the rotation angle of the vertebral body with an X-ray AP image.

In this study, the reference body structure used to evaluate the rotation of the spine in the 2D X-ray image was the pedicle. This is because the pedicle is a structure with less morphological distortion in the structure of the spine. In addition, its positional change can be observed more clearly than other structures in the human body when the spine is rotated, similar to a Scotty dog sign, in general X-ray examination [30,31]. For this reason, in a previous study [32], the pedicle was used as a reference structure in evaluating the internal rotation of the spine. We also obtained data based on the pedicle from the image reconstructed with X-rays by artificially rotating the spine to the patient's long axis (Z-axis) using Xelis software. The degree of rotation of eight different angles of the spine in one vertebra could be obtained by first measuring the RSAA from the axial image in the CT image and calculating the angle at which the vertebrae were artificially rotated to the left and right (Figure 3). However, this method has a limitation in that it shows a lower spatial resolution than general X-ray imaging. As shown in Figure 3, although general X-ray images can produce sharp images through various techniques, images projected through CT cannot produce sharp images. Therefore, we excluded the raw data when it was impossible to obtain a clear anatomical image from the reconstructed X-ray image during the data acquisition process.

We applied a total of 24 regression learning methods using MATLAB software and performed learning with the acquired data, and finally, the Gauss process regression method showed the lowest RMSE value. The RMSE value of the predictive model was 2.74, meaning that it showed a measurement error value of 2.74 degrees in the variable range. These contents were also confirmed in the reproducibility experiment. When X-rays were obtained with the phantom of the human body tilted by 16 degrees, the prediction model result was 13.72 degrees, showing an error of approximately 2.3 degrees. In other words, the internal rotation angle of the spine can be predicted within the RMSE range of the prediction model we developed. Although it does not show a more accurate prediction value, it can be sufficiently applied to patients to observe the course of symptoms after surgery without CT examination. In addition, its utility value is high considering the advantage of providing quantified values in follow-up checks on post-operation. In addition, the left and the right length of the spine, the left and right length of the pedicle, and the spine's height represent the overall size of the spine. Thus, the subject's body size does not limit the use of the developed predictive model. However, this study has limitations. Firstly, In this study, data were acquired by applying T-spine three onwards. This is because there is a high possibility of error in the measurement method proposed by our research group when the size of the spine is small. Secondly, in actual clinical practice, the spine is rotated and expressed in the image when X-ray AP projection is performed in the patient's internally rotated posture. In other words, if the accurate AP projection is not performed, an error in the rotation of the spine may occur when applying the rotation model developed in this study. Additional studies on correction through other X-ray planes are needed to overcome these limitations. Lastly, as mentioned earlier, the RMSE value of the prediction model was 2.74, which showed an error of up to 6.52% in the reference angle we used as raw data. Therefore, it is unreasonable to use it as an accurate indicator for surgical operation because it has not been evaluated whether this tolerance falls within the allowable range in pedicle screw surgery.

5. Conclusions

We developed a predictive model that could evaluate the interramal rotation of the spine based on the image data projected by the rotation of the pedicle by rotating the spine using the virtual multi-projection method through CT image. Its RMSE was 2.74 degrees within 40 degrees, which was 20 degrees on the left and right sides of the rotation range of the spine. The predictive model developed in this study could be used sufficiently for follow-up of patients with scoliosis.

Author Contributions: All authors were actively involved in the study in different capacities writing—original draft preparation, S.-M.Y.; writing—review and editing, T.-S.K.; investigation and measurement visualization, T.-S.K. and S.-M.Y. All authors have read and agreed to the published version of the manuscript.

Funding: This study was supported by the Basic Science Research Program through the National Research Foundation of Korea (NRF), funded by the Ministry of Science, ICT & Future Planning (Grant No. 2018R1D1A1A02085800 and 2021R1F1A1056078).

Institutional Review Board Statement: This study was approved by our Bioethics Committee (approval number: GU-2017-HRa-06-02).

Informed Consent Statement: Informed consent was obtained from all subjects involved in the study.

Data Availability Statement: Not applicable.

Conflicts of Interest: The authors declare no conflict of interest.

References

1. Altaf, F.; Gibson, A.; Dannawi, Z.; Noordeen, H. Adolescent idiopathic scoliosis. *BMJ* **2013**, *346*, f2508. [CrossRef] [PubMed]
2. Aebi, M. The adult scoliosis. *Eur. Spine J.* **2005**, *14*, 925–948. [CrossRef] [PubMed]
3. Chopra, S.; Larson, A.N.; Kaufman, K.R.; Milbrandt, T.A. Accelerometer based assessment of daily physical activity and sedentary time in adolescents with idiopathic scoliosis. *PLoS ONE* **2020**, *15*, e0238181. [CrossRef] [PubMed]
4. Machida, M. Cause of idiopathic scoliosis. *Spine* **1999**, *24*, 2576. [CrossRef] [PubMed]
5. Popko, J.; Kwiatkowski, M.; Gałczyk, M. Scoliosis: Review of diagnosis and treatment. *Pol. J. Appl. Sci.* **2018**, *4*, 31–35.
6. Janicki, J.A.; Alman, B. Scoliosis: Review of diagnosis and treatment. *Paediatr. Child Health* **2007**, *12*, 771–776. [CrossRef]
7. McCance, S.E.; Denis, F.; Lonstein, J.E.; Winter, R.B. Coronal and sagittal balance in surgically treated adolescent idiopathic scoliosis with the King II curve pattern: A review of 67 consecutive cases having selective thoracic arthrodesis. *Spine* **1998**, *23*, 2063–2073. [CrossRef]
8. Morrissy, R.T.; Goldsmith, G.S.; Hall, E.C.; Kehl, D.; Cowie, G.H. Measurement of the Cobb angle on radiographs of patients who have. *J. Bone Jt. Surg. Am.* **1990**, *72*, 320–327. [CrossRef]
9. Brink, R.C.; Homans, J.F.; Schlösser, T.P.; van Stralen, M.; Vincken, K.L.; Shi, L.; Chu, W.C.; Viergever, M.A.; Castelein, R.M.; Cheng, J.C. CT-based study of vertebral and intravertebral rotation in right thoracic adolescent idiopathic scoliosis. *Eur. Spine J.* **2019**, *28*, 3044–3052. [CrossRef]
10. Courvoisier, A.; Drevelle, X.; Vialle, R.; Dubousset, J.; Skalli, W. 3D analysis of brace treatment in idiopathic scoliosis. *Eur. Spine J.* **2013**, *22*, 2449–2455. [CrossRef]
11. Lechner, R.; Putzer, D.; Dammerer, D.; Liebensteiner, M.; Bach, C.; Thaler, M. Comparison of two-and three-dimensional measurement of the Cobb angle in scoliosis. *Int. Orthop.* **2017**, *41*, 957–962. [CrossRef] [PubMed]
12. Tauchi, R.; Tsuji, T.; Cahill, P.J.; Flynn, J.M.; Glotzbecker, M.; El-Hawary, R.; Heflin, J.A.; Imagama, S.; Joshi, A.P.; Nohara, A. Reliability analysis of Cobb angle measurements of congenital scoliosis using X-ray and 3D-CT images. *Eur. J. Orthop. Surg. Traumatol.* **2016**, *26*, 53–57. [CrossRef] [PubMed]
13. Langensiepen, S.; Semler, O.; Sobottke, R.; Fricke, O.; Franklin, J.; Schönau, E.; Eysel, P. Measuring procedures to determine the Cobb angle in idiopathic scoliosis: A systematic review. *Eur. Spine J.* **2013**, *22*, 2360–2371. [CrossRef] [PubMed]
14. Medica, E.M. Brace treatment of Idiopathic Scoliosis is effective for a curve over 40 degrees, but is the evaluation of Cobb angle the only parameter for the indication of treatment? *Eur. J. Phys. Rehabil. Med.* **2019**, *55*, 231–240.
15. Shaw, M.; Adam, C.J.; Izatt, M.T.; Licina, P.; Askin, G.N. Use of the iPhone for Cobb angle measurement in scoliosis. *Eur. Spine J.* **2012**, *21*, 1062–1068. [CrossRef]
16. Ho, E.K.; Upadhyay, S.S.; Chan, F.L.; Hsu, L.C.; Leong, J.C. New methods of measuring vertebral rotation from computed tomographic scans. An intraobserver and interobserver study on girls with scoliosis. *Spine* **1993**, *18*, 1173–1177. [CrossRef]
17. Vavruch, L.; Forsberg, D.; Dahlström, N.; Tropp, H. Vertebral axial asymmetry in adolescent idiopathic scoliosis. *Spine Deform.* **2018**, *6*, 112–120.e1. [CrossRef]
18. Koreska, J.; Gibson, D.A.; Robertson, D. Three-dimensional analysis of spinal deformities. *J. Eng. Mech. Div.* **1978**, *104*, 239–253. [CrossRef]
19. Roaf, R. Rotation movements of the spine with special reference to scoliosis. *J. Bone Jt. Surg. Br. Vol.* **1958**, *40*, 312–332. [CrossRef]
20. Lafage, V.; Leborgne, P.; Mitulescu, A.; Dubousset, J.; Lavaste, F.; Skalli, W. *Comparison of Mechanical Behaviour of Normal and Scoliotic Vertebral Segment: A Preliminary Numerical Approach*; Research into Spinal Deformities 3; IOS Press: Amsterdam, The Netherlands, 2002; pp. 340–344.
21. Beuerlein, M.J.; Raso, V.J.; Hill, D.L.; Moreau, M.J.; Mahood, J.K. The relationship between axial rotation and lateral bending. *Stud. Health Technol. Inform.* **1999**, *9*, 105–108.

22. Kjellberg, M.; Al-Amiry, B.; Englund, E.; Sjödén, G.O.; Sayed-Noor, A.S. Measurement of leg length discrepancy after total hip arthroplasty. The reliability of a plain radiographic method compared to CT-scanogram. *Skelet. Radiol.* **2012**, *41*, 187–191. [CrossRef] [PubMed]
23. Wessberg, P.; Danielson, B.I.; Willén, J. Comparison of Cobb angles in idiopathic scoliosis on standing radiographs and supine axially loaded MRI. *Spine* **2006**, *31*, 3039–3044. [CrossRef] [PubMed]
24. Vock, P. CT dose reduction in children. *Eur. Radiol.* **2005**, *15*, 2330–2340. [CrossRef] [PubMed]
25. Calhoun, P.S.; Kuszyk, B.S.; Heath, D.G.; Carley, J.C.; Fishman, E.K. Three-dimensional volume rendering of spiral CT data: Theory and method. *Radiographics* **1999**, *19*, 745–764. [CrossRef] [PubMed]
26. Sugimoto, Y.; Tanaka, M.; Nakanishi, K.; Misawa, H.; Takigawa, T.; Ozaki, T. Predicting intraoperative vertebral rotation in patients with scoliosis using posterior elements as anatomical landmarks. *Spine* **2007**, *32*, E761–E763. [CrossRef]
27. Delorme, S.; Labelle, H.; Aubin, C.; de Guise, J.A.; Rivard, C.H.; Poitras, B.; Coillard, C.; Dansereau, J. Intraoperative comparison of two instrumentation techniques for the correction of adolescent idiopathic scoliosis: Rod rotation and translation. *Spine* **1999**, *24*, 2011–2017. [CrossRef]
28. Lafon, Y.; Lafage, V.; Dubousset, J.; Skalli, W. Intraoperative three-dimensional correction during rod rotation technique. *Spine* **2009**, *34*, 512–519. [CrossRef]
29. Lam, G.C.; Hill, D.L.; Le, L.H.; Raso, J.V.; Lou, E.H. Vertebral rotation measurement: A summary and comparison of common radiographic and CT methods. *Scoliosis* **2008**, *3*, 16–25. [CrossRef]
30. Perdriolle, R.; Vidal, J. Thoracic idiopathic scoliosis curve evolution and prognosis. *Spine* **1985**, *10*, 785–791. [CrossRef]
31. Drerup, B. Principles of measurement of vertebral rotation from frontal projections of the pedicles. *J. Biomech.* **1984**, *17*, 923–935. [CrossRef]
32. Stokes, I.A.; Bigalow, L.C.; Moreland, M.S. Measurement of axial rotation of vertebrae in scoliosis. *Spine* **1986**, *11*, 213–218. [CrossRef] [PubMed]